INFECTION AND IMMUNITY, Mar. 2006, p. 1777–1785 Vol. 74, No. 3
0019-9567/06/$08.00+0 doi:10.1128/IAI.74.3.1777–1785.2006

Identification of Fibronectin-Binding Proteins in *Mycoplasma gallisepticum* Strain R

Meghan May,[1,2] Leka Papazisi,[3] Timothy S. Gorton,[1,2] and Steven J. Geary[1,2]*

Department of Pathobiology and Veterinary Science[1] and Center of Excellence for Vaccine Research,[2] The University of Connecticut, 61 North Eagleville Rd., Storrs, Connecticut 06269, and The Institute for Genomic Research, 9712 Medical Center Dr., Rockville, Maryland 20850[3]

Received 2 November 2005/Returned for modification 16 November 2005/Accepted 19 November 2005

We have determined that virulent *Mycoplasma gallisepticum* strain R_{low} is capable of binding the extracellular matrix protein fibronectin. Fibronectin was found to be present in *M. gallisepticum* R_{low} protein extracts by Western blotting and peptide sequencing. *Mycoplasma gallisepticum* R_{high}, the attenuated, high-passage derivative of R_{low}, is deficient in this ability. MGA_1199, the *M. gallisepticum* homologue of the cytadherence-associated protein P65 from *Mycoplasma pneumoniae*, and MGA_0928, the *M. gallisepticum* homologue of the *M. pneumoniae* cytoskeletal protein HMW3, were identified as fibronectin-binding proteins. Peptides from the regions of MGA_1199 and MGA_0928 exhibiting the highest degree of homology with known fibronectin-binding proteins were shown to bind the gelatin/heparin-binding domain of fibronectin. MGA_1199 and MGA_0928 were shown to be absent and aberrant, respectively, in R_{high}, explaining its lack of fibronectin-binding capability. Consistent with its *M. pneumoniae* counterpart, MGA_1199 (renamed PlpA) was demonstrated to be surface exposed, despite a lack of classical membrane-spanning domains. Due to its demonstrated topology and the strength of interaction between its binding peptide and fibronectin, we propose that PlpA functions as a fibronectin-binding protein in vivo and may possess atypical transmembrane domains.

The avian pathogen *Mycoplasma gallisepticum* is known to cause chronic respiratory disease in chickens, infectious sinusitis in turkeys, and conjunctivitis in finches (23, 33, 45, 49). The chronic nature of the infection and its effects on weight and egg production render it a pathogen of considerable economic importance to the poultry industry (49). *Mycoplasma gallisepticum*, together with *Mycoplasma pneumoniae* and *Mycoplasma genitalium*, is one of the three most prominent members of the *M. pneumoniae* phylogenetic cluster. Members of this cluster are pathogens that establish chronic infections and mediate attachment to the host epithelium via molecules present on a complex tip structure (33). The proteins that compose the tip structure, as well as a model for its assembly, have been described using *M. pneumoniae* (1, 18, 19).

The virulence of strain R has been previously examined by comparing the virulent, low-passage strain (R_{low}) with the attenuated, high-passage strain (R_{high}) (29). Initial examination of the protein profiles of R_{low} and R_{high} indicated that three proteins were absent in R_{high}. These proteins have been identified as the primary cytadhesin GapA, the cytadherence-related molecule CrmA, and a high-affinity transport protein, HatA (29, 44). Complementation experiments with R_{high} using wild-type *gapA* and *crmA* demonstrated that coexpression of GapA and CrmA is essential for cytadherence in *M. gallisepticum* (27); however, these attachment molecules were not able to completely restore virulence, suggesting that additional differences contribute to the attenuation of the high-passage isolate.

With this in mind, we more closely examined the protein profiles of R_{low} and R_{high} and found that, in addition to GapA, CrmA, and HatA, R_{high} is deficient in two high-molecular-mass proteins and expresses an aberrant form of a third protein. We identify two of these proteins as being encoded by MGA_0928 and MGA_1199 and characterize these as homologues of the *M. pneumoniae* tip structure proteins, HMW3 and P65, respectively. In accordance with standard nomenclature, we henceforth refer to these proteins of *M. gallisepticum* as HMW3-like protein (Hlp3) and *pneumoniae*-like protein A (PlpA).

The third protein was identified as the extracellular matrix protein fibronectin, which led us to believe that *M. gallisepticum* R_{low} was capable of binding fibronectin from the growth medium and that one or both of the high-molecular-mass proteins Hlp3 and PlpA were responsible for this binding. Many pathogens, including *M. pneumoniae* (7), are known to bind components of the extracellular matrix for various reasons. Some bacteria utilize this ability to evade the immune system of their host (9), to mediate cytadherence (41, 42), to initiate biofilm formation (13, 37), or to attach to and invade host cells (8, 26, 34, 38, 40). In addition to these activities by bacteria, fibronectin binding has been shown to play a role in the hematogenous spread of cancer cells (4, 46).

We present below the identification of two proteins believed to be involved in cytoskeletal and tip structure formation and demonstrate their roles in fibronectin binding. In the absence of classical transmembrane domains, we present evidence to suggest that PlpA utilizes atypical domains to anchor itself within the membrane. Although the current study does not formally address the role of fibronectin binding in the virulence of R_{low}, the ability to bind fibronectin is advantageous to other

* Corresponding author. Mailing address: Department of Pathobiology and Veterinary Science, University of Connecticut, 61 North Eagleville Rd., Storrs, CT 06269. Phone: (860) 486-0835. Fax: (860) 486-2794. E-mail: geary@uconnvm.uconn.edu.

TABLE 1. Primer sequences and descriptions

Primer name	Sequence (5′–3′)	Description
SG1083	ACCAAACGAACTAAATCTTTTAATTGACA	*hlp3* forward
SG1084	GGTGAATAGTTCGTATGCTTGAT	*hlp3* reverse
SG1090.5	CAACAACCAAGAGTGCGAAG	*hlp3* (RT) forward
SG1097	AACCCGTTGTGAATTGGTTC	*hlp3* (RT) reverse
SG1182	AATCAACCTGGACAACAAGG	*plpA* forward
SG1183	TAACGGTTATTGTAAGGGTC	*plpA* reverse
SG1187	CAACCTGACTATTACAG	*plpA* (RT) forward
SG1188	GTAGCCATCGTCAAATCCAG	*plpA* (RT) reverse

pathogens and thus can be considered a potential component of virulence in R_{low}.

MATERIALS AND METHODS

***M. gallisepticum* strains and growth conditions.** *M. gallisepticum* strains R_{low} (passage 14) and R_{high} (passage 164) (29) were grown in complete Hayflick's medium at 37°C. OneShot *Escherichia coli* DH5α (Invitrogen, Carlsbad, CA) was grown in LB broth containing 50-μg/ml ampicillin at 37°C.

SDS-PAGE and peptide sequencing. Sodium dodecyl sulfate-polyacrylamide gel electrophoresis (SDS-PAGE) was performed as described by Laemmli (21). Proteins were extracted by Triton X-114 phase partitioning as described by Bordier (3). Triton X-114-insoluble proteins were solubilized in 10% sodium dodecyl sulfate. All protein phases were stored at −20°C prior to separation in 5% polyacrylamide gels. Proteins found to be present in R_{low} and absent in R_{high} were subjected to in-gel digestion and matrix-assisted laser desorption ionization–mass spectrometry (MALDI-MS) analysis (14) (Molecular Structure Facility, University of California, Davis, CA). The resulting amino acid data were aligned with the *M. gallisepticum* strain R proteome using the FastA program (31).

Generation of antisera. Peptides were designed for the generation of antisera against PlpA and Hlp3 (see below). These peptides were synthesized and conjugated to keyhole limpet hemocyanin (KLH) (Sigma-Genosys, The Woodlands, Tex.). Peptides-KLH conjugates were coupled with complete Freund's adjuvant and used to immunize New Zealand White rabbits. Rabbits were boosted with KLH-conjugated peptide in the presence of incomplete Freund's adjuvant at 2-week intervals. After 8 weeks, rabbits were exsanguinated, and the sera were separated and stored at −80°C. The process of generating antisera was performed in its entirety by Sigma-Genosys.

Western blots. Triton X-114-insoluble phase proteins from *M. gallisepticum* were separated by SDS-PAGE and transferred to nitrocellulose membranes (43). Membranes were blocked with 5% bovine serum albumin or skim milk for 1 h at 37°C. Membranes were then reacted with primary antibody, either rabbit anti-fibronectin (Rockland Immunochemicals, Gilbertsville, PA), rabbit anti-PlpA, or rabbit anti-HMW3 (47) (kindly provided by Duncan Krause, The University of Georgia, Athens, GA) at dilutions of 1:8,000, 1:1,000, and 1:5,000, respectively, and incubated for 12 h at 4°C. Horseradish peroxidase-conjugated goat anti-rabbit immunoglobulin G (IgG) (Kirkegaard and Perry Laboratories, Gaithersburg, MD) was added at a dilution of 1:7,000 and incubated for 2 h at 37°C. Blots were developed with the 4-chloro-1-naphthol–hydrogen peroxide chromogenic substrate.

Nucleic acid extraction. Genomic DNA was isolated from R_{low} and R_{high} using the Easy DNA kit (Invitrogen) according to the manufacturer's instructions. RNA was extracted from R_{low} and R_{high} with TRIzol reagent (Invitrogen) according to the manufacturer's instructions and stored in 5-μg aliquots at −70°C. Aliquots of RNA were thawed as needed and treated with DNase I (Invitrogen) according to the manufacturer's instructions.

PCR conditions. PCR amplifications of *plpA* and *hlp3* were performed using the Expand Hi Fidelity PCR System (Roche Applied Science, Indianapolis, IN) according to the manufacturer's specifications. Each PCR contained 100 ng genomic DNA and dinucleotide triphosphates at a final concentration of 200 μM. Primers SG1083 and SG1084 (*hlp3*) and SG1182 and SG1183 (*plpA*) (MWG Biotech, Raleigh, NC) (Table 1) were used at a final concentration of 10 μM. Initial denaturation of DNA was accomplished at 94°C for 2 min. Initial amplification was achieved by 10 cycles of the following: denaturation at 94°C for 20 s, primer annealing at 48°C for 30 s, and extension at 71°C for 5 min. Twenty additional cycles were performed, during which 5 s per cycle was added to the extension time. A final extension of 10 min was performed at 71°C.

Nucleotide sequencing. PCR amplicons were cloned into pCR2.1 (Invitrogen) according to the manufacturer's instructions. Recombinant plasmids were chemically transformed into OneShot *Escherichia coli* (Invitrogen) according to the manufacturer's instructions for propagation. DNA sequencing was accomplished by primer walking and was performed at the University of Connecticut Bioscience Center (Storrs, CT) using ABI BigDye (Applied Biosystems, Norwalk, CT) and the ABI Prism 373 DNA Sequencer (Applied Biosystems). DNA sequence assembly and analysis were performed using Sequencher (Gene Codes Corporation, MI).

Transcriptional analysis by RT-PCR. Transcriptional analysis was performed by reverse transcriptase PCR (RT-PCR) using 1.7 μg RNA per reaction mixture. Amplifications were performed using the SuperScript RT-PCR kit (Invitrogen) according to the manufacturer's instructions. Reverse transcription was accomplished by incubation of RNA in SuperScript reaction mixture at 50°C for 25 min. cDNA was denatured for 2 min at 94°C and then amplified by 35 cycles of the following parameters: denaturation at 94°C for 20 s, primer annealing at 49°C for 30 s, and extension at 72°C for 1 min. A final extension of 10 min was performed at 72°C. A 500-bp fragment from the 3′ end of *hlp3* was amplified using the primers SG1090.5 and SG1097 (Table 1). A 250-bp fragment was amplified from the 3′ end of *plpA* using primers SG1187 and SG1188 (Table 1). RNA was examined for DNA contamination by substituting Ampli*Taq* DNA polymerase (Applied BioSystems) for the SuperScript Platinum *Taq* under identical amplification conditions.

Peptide design and generation. Kyte-Doolittle hydrophobicity plots (20) were used to identify antigenic peptides (Table 2) from the protein sequences of PlpA and Hlp3 for the generation of antisera (Sigma-Genosys). Protein sequence alignments between PlpA, Hlp3, and annotated fibronectin-binding proteins (e.g., GenBank accession numbers ZP_00144610, CAA44726, NP_801368, NP_764439, A41461, B64235, AAP10794, and BAB81553) were performed using AlignX Blocks (InforMax/Invitrogen). Peptides representing the most homologous regions (see Fig. 4B) were generated by the American Peptide Company (San Francisco, CA). Peptides representing the membrane protein-associated motifs GG_4 (GxxxG), II_4 (IxxxI), an expanded motif of GG_4 (GxxxGxxxG) as it appears in PlpA, and control peptides were generated by Sigma-Genosys. The N-terminal residue of each peptide was labeled with biotin.

Peptide-binding assay. Bovine fibronectin (Calbiochem, San Diego, CA) or one of four subunits of human fibronectin—fragment IIIC (Sigma, St. Louis, MO), the adhesion-promoting peptide (Sigma), residues 1377 to 1398 (Sigma), or the gelatin/heparin-binding domain (Sigma)—were separated by SDS-PAGE and transferred to nitrocellulose membranes as previously described. The degree of sequence homology between bovine, human, and chicken fibronectin renders them experimentally interchangeable. Membranes were blocked with skim milk

TABLE 2. Peptide sequences[a]

Peptide name	Sequence	Motif	Purpose
GG_4	^{btn}NGMLAGV	GxxxG	Putative transmembrane peptide
II_4	^{btn}QIPVVIK	IxxxI	Putative transmembrane peptide
GG_4E	^{btn}YGNPIGMLPG	GyxxGxxxG	Putative transmembrane peptide
Ponticulin	^{btn}TTSYIVSC	Undefined	Transmembrane control +
PlpA$^-$	^{btn}DEKKPRNKK	yyyyxyyyy	Transmembrane control −
PlpA-CTD	^{KLH}CIQPSFRRRGGRAKF	NA	Antiserum generation
PlpA-MID	^{KLH}APVHYDENEELSTDDL	NA	Antiserum generation
Hlp3-CTD	^{KLH}GYDYDRPSTQYYRSN	NA	Antiserum generation

[a] Peptide names, sequences, motifs, sources, and experimental roles are listed. Motif spaces indicated with an x represent nonpolar amino acids, whereas those indicated with a y represent polar or charged residues.

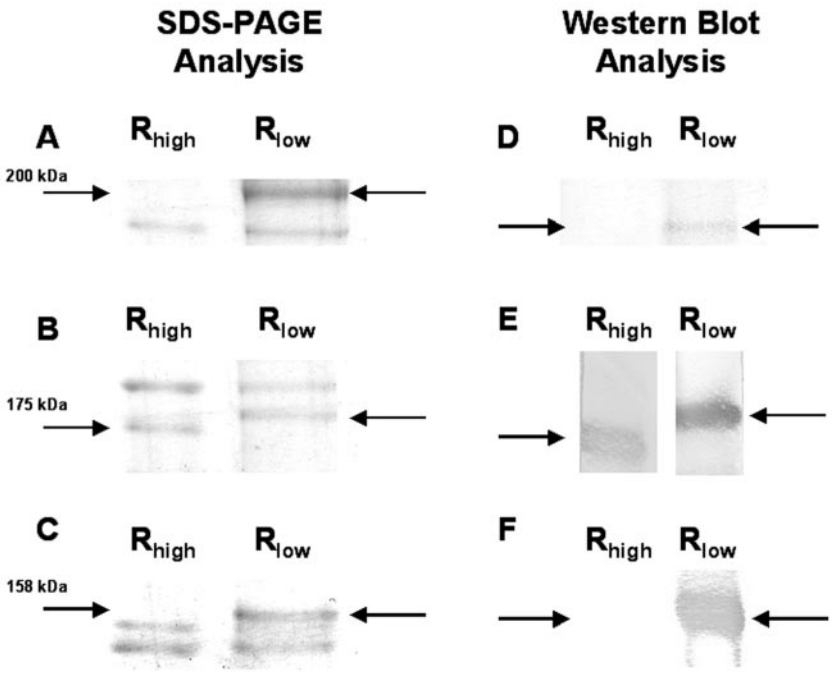

FIG. 1. Protein profiles of R_{low} and R_{high} analyzed by SDS-PAGE and Western blotting. SDS-PAGE (A, B, and C) and Western blotting (D, E, and F) demonstrate that three proteins were clearly absent (A, C, D, and F) or aberrant (D and E) in R_{high}. Arrows indicate the presence or absence of the implicated proteins, and pertinent molecular masses are noted. Western blot analysis was performed with anti-fibronectin (D), anti-HMW3 (E), and anti-PlpA (F).

for 1 h at 37°C and incubated in solutions containing 1 mg/ml putative fibronectin-binding peptide in phosphate-buffered saline (PBS) at 4°C for 12 h. Following three washes with phosphate-buffered saline–0.005% Tween 20, bound peptides were detected with horseradish peroxidase-conjugated streptavidin (2 μg/ml). Blots were developed with the 4-chloro-1-naphthol–hydrogen peroxide chromogenic substrate.

Binding inhibition assay. IgG molecules were separated from other serum components of anti-PlpA antiserum and normal rabbit serum using the Immuno-Pure Protein G column (Pierce, Rockford, IL) according to the manufacturer's instructions. Four micrograms of bovine fibronectin (Calbiochem) was placed into each well of a 96-well polystyrene microtiter plate (Immulon 4HBX; Thermo Electron Corporation, Milford, MA) and incubated at 37°C for 1 h. All wells were blocked with 5% bovine serum albumin for 1 h at 37°C. *Mycoplasma gallisepticum* R_{low} cells from 1 ml of a mid-log-phase culture were harvested by centrifugation (15,000 × *g* for 10 min) and washed three times in phosphate-buffered saline. Solutions containing 10^7 CFU, 10^5 CFU, and 10^3 CFU were preincubated for 1 h at 37°C with 3 μg of either anti-PlpA IgG or normal rabbit serum IgG, added to fibronectin-coated wells, and incubated for 1 h at 37°C. Unbound cells were removed by being washed three times with PBS–0.005% Tween 20. Bound organisms were detected by incubation with chicken anti-*M. gallisepticum* at a dilution of 1:5,000, followed by horseradish peroxidase-conjugated goat anti-chicken (Kirkegaard and Perry Laboratories) at a dilution of 1:2,000. Peroxidase activity was visualized by the addition of phosphate-citrate buffer containing hydrogen peroxide and *o*-phenylenediamine. Absorbance was measured at 460 nm. Statistical significance was determined by Student's *t* test using the SAS statistical analysis program, version 8.01 (SAS Institute, Cary, NC).

Surface proteolysis assay. Eight 2-ml aliquots of an R_{low} mid-log-phase culture were harvested by centrifugation (15,000 × *g* for 10 min) and washed three times with PBS. Five of the pellets were each exposed to 7.0 μg of proteinase K (QIAGEN, Inc., Valencia, CA) at 42°C for intervals of 15, 30, 45, 60, or 300 s. After incubation, proteinase K activity was inhibited by the addition of phenylmethylsulfonyl fluoride (PMSF) to a final concentration of 10 mM. The sixth pellet was resuspended in 0.1% Triton X-114 (to allow for the degradation of all protein) and incubated with proteinase K for 300 s prior to the addition of PMSF. The seventh pellet was simultaneously exposed to proteinase K and PMSF to neutralize any proteolytic activity and to serve as a zero time point. The eighth cell pellet was left untreated. Proteins from the eight cell pellets were then separated by SDS-PAGE and Western blotted as described above with anti-PlpA serum.

Growth inhibition by complement-mediated lysis. *Mycoplasma gallisepticum* R_{low} and R_{high} cultures (approximately 10^8 cells) were pelleted and washed three times with PBS. Cell pellets were resuspended in a solution of 75% guinea pig serum (serving as a source of complement components), 12.5% hyperimmune rabbit serum raised against the PlpA midsection (MID) peptide (Table 2), and 12.5% hyperimmune rabbit serum raised against the PlpA carboxy-terminal (CTD) peptide (Table 2). One R_{low} cell pellet was resuspended in 100% guinea pig serum to serve as a standard for comparison. Cells in serum suspensions were gently shaken in an orbital incubator at 50 rpm for a period of 2 h at 37°C. Complete Hayflick's medium was added to the suspension, and cells were incubated for 24 h at 37°C. Following incubation, optical density measurements were taken (λ = 620 nm). Cell growth was considered an indication of viability and therefore a lack of complement-mediated lysis; cell growth was assessed by a positive change in optical density. Statistical significance was determined by analysis of variance using the SAS statistical analysis program, version 8.01 (SAS Institute).

Peptide incorporation into liposomes. Liposomes were generated according to the method of Avanti Polar Lipids as originally developed by Morrissey (25). Briefly, a solution of 32.5 mM phosphatidylcholine-chloroform, 32.5 mM phosphatidylethanolamine-chloroform, and 12.4 mM phosphatidylserine-chloroform (40:40:20 molar ratio) (Avanti Polar Lipids, Alabaster, AL) was generated in the presence of 100 μg of each membrane-associated peptide (i.e., GxxxG, IxxxI, and GxxxGxxxG [in dimethyl sulfoxide] and controls [in water]). Dry nitrogen gas was used to evaporate the chloroform-water supernatant. Liposomes were further dried under a vacuum for 60 min at 30°C, then washed three times with PBS, and incubated in 2-μg/ml horseradish-peroxidase-conjugated streptavidin (Pierce) for 12 h at 4°C. Following incubation, liposomes were washed three times with PBS, then dissolved in chloroform, and immobilized on paraffin wax for visualization of signal. Bound streptavidin was visualized by development in the 4-chloro-1-naphthol–hydrogen peroxide chromogenic substrate.

Embedding of peptides into *M. gallisepticum* cell membranes. *Mycoplasma gallisepticum* R_{low} cells were made electrocompetent as previously described (28), mixed with 100 μg of each membrane-associated peptide in a 0.1-mm cuvette (Bio-Rad, Hercules, CA), and electroporated at 2.5 kV (GenePulser II; Bio-Rad). Nonpulsed controls for each peptide were also included to exclude the

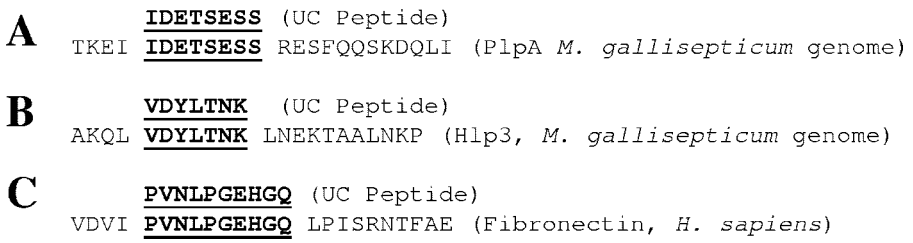

FIG. 2. Sample peptide alignments. (A) Peptides generated from MALDI-MS analysis of the 158-kDa band aligned with PlpA. (B and C) Peptides generated from the 200-kDa band aligned with Hlp3 or with fibronectin.

possibility of peptides binding the cell surface nonspecifically. Cells were allowed to recover for 120 min in Hayflick's medium at 37°C. Cells were washed three times with PBS, resuspended in 25 μl PBS, and spotted onto nitrocellulose membranes. Membranes were blocked with 5% dry milk in water for 1 h at 37°C and incubated in horseradish peroxidase-conjugated streptavidin for 12 h at 4°C. Bound streptavidin was visualized by development in the 4-chloro-1-naphthol–hydrogen peroxide chromogenic substrate.

RESULTS

Peptide sequencing. As shown in Fig. 1A and C, two high-molecular-mass proteins were absent from R_{high} that are present in R_{low}, and a third appeared to run at an aberrant molecular mass in R_{high} (Fig. 1E). MALDI-MS analysis performed on the 200-kDa (Fig. 1A) protein band produced peptides that aligned with the homologue of the *M. pneumoniae* cytoskeletal protein HMW3 (Hlp3) and the eukaryotic extracellular matrix protein fibronectin. MALDI-MS analysis performed on the 158-kDa protein (Fig. 1C) produced peptides that aligned with PlpA, the homologue of the *M. pneumoniae* cytadherence-associated protein P65. The protein bands that appeared to be of differing molecular masses in R_{low} (Fig. 1B) were also identified as Hlp3 by N-terminal sequence analysis of R_{low} and R_{high}, indicating that the presence of Hlp3 in the 200-kDa band represented binding rather than simple comigration. These alignments are shown in Fig. 2A to C.

Western blots. Blots of Triton X-114-insoluble-phase proteins extracted from R_{low} were positive when reacted with anti-fibronectin and anti-PlpA antibodies (Fig. 1D and F), while blots of insoluble-phase proteins from R_{high} were negative (Fig. 1D and F). Blots of insoluble-phase proteins from R_{high} were weakly reactive to antibodies raised against the *M. pneumoniae* homologue of Hlp3 (HMW3), while blots of insoluble-phase proteins from R_{low} were strongly positive (Fig. 1E).

Nucleotide sequencing of *hlp3* and *plpA*. Nucleotide sequencing of *hlp3* from R_{high} showed a 54-bp deletion at base 816 of 3252 (Fig. 3A). Nucleotide sequencing of *plpA* from R_{high} showed a 17-bp insertion at base 2070 of 2568 that results in a frameshift mutation and subsequently a premature stop codon at base 2206 of 2568 (Fig. 3B).

Transcriptional analysis by RT-PCR. RT-PCR indicated that transcripts for *hlp3* and *plpA* were produced in both R_{low} and R_{high} (data not shown).

Peptide-binding assays. Peptides 1 (Hlp3) and 7 (PlpA) (Fig. 4B) were shown to bind immobilized fibronectin (Fig. 5A and B). The strongest interaction was between fibronectin and peptide 7. Amino acid comparisons of peptides 1 and 7 demonstrate 60% identity and 80% similarity (Fig. 4C). Peptide 7 was shown to bind the gelatin/heparin-binding domain of fibronectin (Fig. 5C).

Binding inhibition assay. Whole R_{low} cells preincubated with normal rabbit serum IgG were found to bind fibronectin at a significantly ($P < 0.02$) higher level than R_{low} cells preincubated with anti-PlpA IgG (Fig. 6).

Surface proteolysis assay. Protein was shown to be present in all samples not treated with Triton X-114 after treatment with proteinase K for up to 300 s. Untreated cell pellets and cell pellets treated with proteinase K for 0 or 15 s reacted with anti-PlpA serum. All cell pellets treated with proteinase K for 30 s or longer were not reactive to anti-PlpA serum, indicating that PlpA was degraded (data not shown).

Growth inhibition by complement-mediated lysis assay. Incubation of R_{low} cells in anti-PlpA serum in the presence of complement components significantly ($P < 0.004$) inhibited their growth upon incubation in Hayflick's medium compared to R_{low} cells incubated in complement compo-

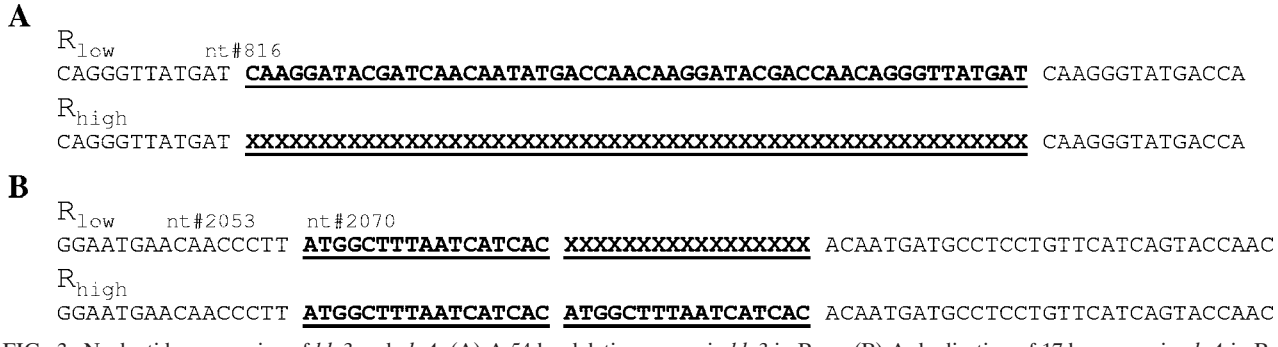

FIG. 3. Nucleotide sequencing of *hlp3* and *plpA*. (A) A 54-bp deletion occurs in *hlp3* in R_{high}. (B) A duplication of 17 bp occurs in *plpA* in R_{high}.

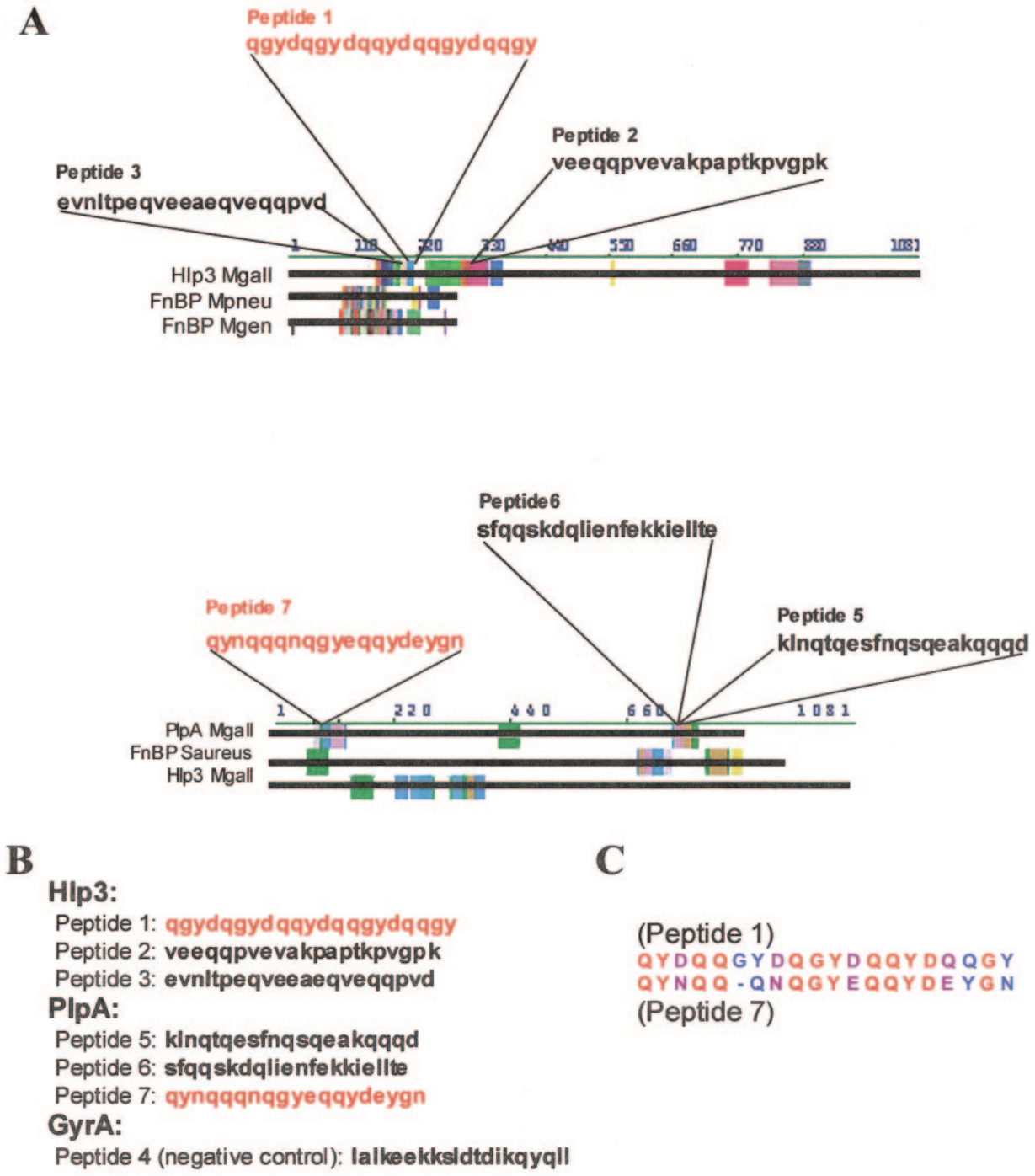

FIG. 4. Suspected fibronectin-binding peptides. (A) AlignX Blocks was used to define homologous regions between PlpA, Hlp3, and known fibronectin-binding proteins. (B) Peptides derived from the most homologous regions of each block are shown. Peptides shown to bind fibronectin are displayed in red. (C) Peptides 1 (Hlp3) and 7 (PlpA) are aligned. Identical amino acids are shown in red, similar amino acids are shown in purple, and dissimilar amino acids are shown in blue. These peptides, each shown to bind fibronectin, are 60% identical and 80% similar.

nents alone (Fig. 7). This inhibition of growth was considered an indication of complement-mediated lysis.

Investigation of putative transmembrane regions. Bound streptavidin was considered an indication of embedded peptide. GxxxG and IxxxI peptides did not interact with or embed within liposomes (Fig. 8A) or *M. gallisepticum* membranes (Fig. 8B). A peptide representing the expanded motif of GxxxG (i.e., GxxxGxxxG) embedded within liposomes (Fig. 8A), appearing in a globular pattern due to the spotting of liposomes on paraffin wax. The expanded motif peptide also embedded within *M. gallisepticum* membranes and did not bind the cell surface nonspecifically (Fig. 8B). A hydrophilic peptide

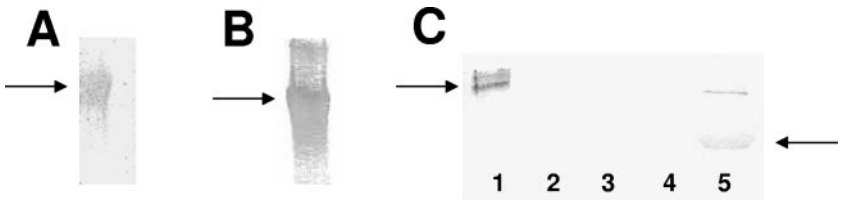

FIG. 5. Peptide-binding assays. Biotinylated peptides from the homologous blocks were shown to bind fibronectin immobilized on nitrocellulose, as indicated by arrows. Peptide 1 from Hlp3 (A) and peptide 7 from PlpA (B) were both shown to bind. These peptides were 60% identical and 80% similar to each other. (C) Peptide 7 was exposed to immobilized subunits of fibronectin and shown to interact with the gelatin/heparin-binding domain. Lane 1, whole fibronectin; lane 2, fragment IIIC; lane 3, adhesion-promoting peptide; lane 4, residues 1377 to 1398; lane 5, gelatin/heparin-binding domain.

from PlpA ($PlpA^-$) that served as a negative control did not embed in either liposomes or *M. gallisepticum* membranes (Fig. 8A and B). A peptide representing a suspected atypical membrane-spanning region from the *Dictyostelium discoideum* protein ponticulin that served as a positive control was shown to incorporate into liposomes. This peptide appeared to bind the *M. gallisepticum* surface nonspecifically, making evaluation of its embedding impossible (Fig. 8A and B).

DISCUSSION

We have demonstrated that in addition to the previously characterized cytadhesin molecules GapA and CrmA and the ABC transporter HatA (29), *M. gallisepticum* strain R_{high} does not express PlpA, expresses an aberrant form of Hlp3, and does not contain the extracellular matrix protein fibronectin in protein profiles. As *M. gallisepticum* does not encode any molecules with sequence homology to fibronectin (28), we concluded that the virulent *M. gallisepticum* strain R_{low} is capable of binding fibronectin, while the avirulent strain R_{high} is impaired in this ability.

Amino acid sequence data for the 200-kDa band present in R_{low} but not R_{high} identified both Hlp3 and fibronectin. Hlp3 (with an observed molecular mass of 175 kDa) bound to a fibronectin monomer (with an observed molecular mass of 200 kDa) would be expected to run at approximately 375 kDa in SDS-PAGE. Therefore, the observed size of 200 kDa for the bound complex of Hlp3 and fibronectin may possibly be due to fragments of fibronectin being bound to full-length Hlp3, fragments of Hlp3 being bound to a complete fibronectin monomer, or fragments of both proteins creating a smaller-than-expected protein complex. We have not yet explored the phenomenon of these two proteins existing in what appears to

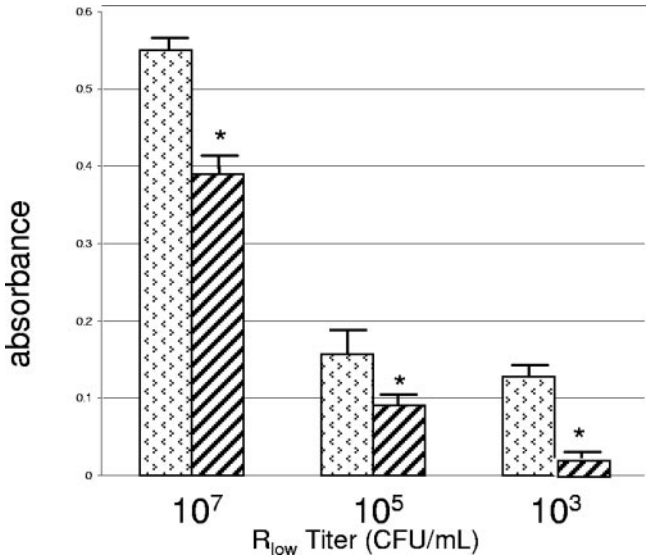

FIG. 6. Binding inhibition assay to demonstrate surface exposure of PlpA. Decreasing titers of R_{low} were incubated with preimmune rabbit serum IgG (stippled bars) and with anti-PlpA IgG (striped bars) and then exposed to immobilized fibronectin in microtiter plates. Bound organisms were detected by chicken anti-R_{high}, followed by horseradish peroxidase (HRP)-conjugated goat anti-chicken. At each titer, a significant difference (*) ($P < 0.02$) in the level of colorimetric signal (*o*-phenylenediamine) generated was observed.

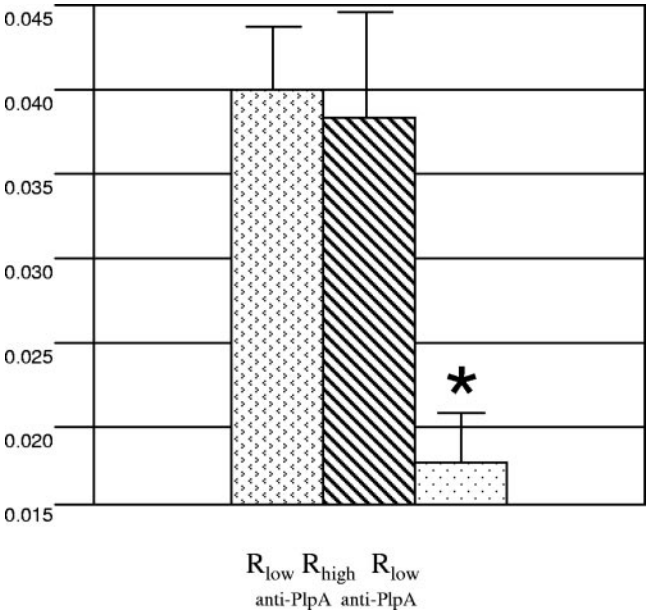

FIG. 7. Growth inhibition by complement-mediated lysis. R_{low} cells were incubated in the presence of hyperimmune rabbit serum raised against the MID and CTD of PlpA and guinea pig serum or in guinea pig serum alone. Following incubation at 37°C, Hayflick's medium was added. Growth of R_{low} was assessed by optical density after 24 h. Incubation in the presence of complement components and anti-PlpA antiserum significantly ($P < 0.004$) impeded the subsequent growth of R_{low} (spotted bars) compared to the growth of R_{high} (striped bars) incubated in the presence of anti-PlpA antiserum and complement components or R_{low} (stippled bars) incubated in the presence of complement components alone.

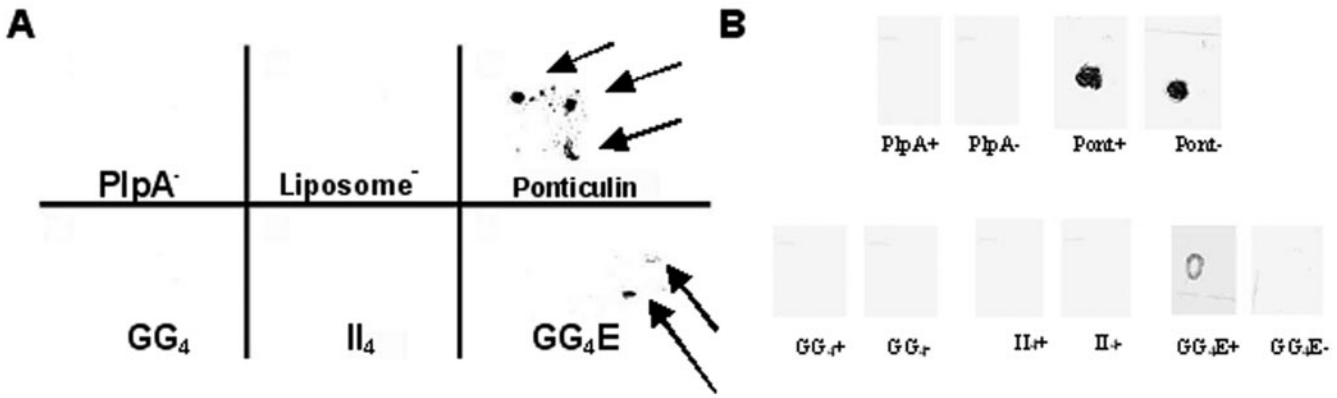

FIG. 8. Investigation of putative transmembrane regions of PlpA. GxxxG (GG_4), IxxxI (II_4), and GxxxGxxxG (GG_4E) motifs from PlpA were examined for their abilities to interact with membranes. Liposomes were generated in the presence of biotinylated peptides representing these motifs. Excess peptide was removed by washing. Liposomes were immobilized on paraffin wax, after which incorporated peptides were detected with streptavidin-HRP. (A) Empty liposomes, the hydrophilic peptide ($PlpA^-$), the GG_4 peptide, and the II_4 peptide did not show any reactivity, indicating that no peptide was incorporated during synthesis. The ponticulin peptide and the expanded motif of GG_4 did show reactivity (arrows), indicating that they were incorporated into the liposomes. In addition, biotinylated peptides were introduced into the membrane of *M. gallisepticum* by electroporation. Resulting cells were spotted onto nitrocellulose for the detection of embedded peptide by streptavidin-HRP. (B) Panels are labeled with the name of each peptide; those marked with a plus sign represent electroporated cells used to detect embedding, and those marked with a minus sign represent nonpulsed cells mixed with peptides to detect nonspecific binding. The hydrophilic peptide ($PlpA^-$), the GG_4 peptide, and the II_4 peptide did not embed in the membrane or bind to it nonspecifically. The ponticulin peptide embedded in the membrane but also bound the cell surface nonspecifically. The expanded repeat of GG_4 embedded in the cell membrane and did not bind nonspecifically.

be a complexed state in a denaturing gel; however, these fortuitous observations led us to further investigate the fibronectin-binding capabilities of *M. gallisepticum*. Due to the observed homology between Hlp3 and PlpA, as well as the absence of PlpA from R_{high}, the fibronectin-binding capabilities of both Hlp3 and PlpA are described in this paper.

The presence of fibronectin and PlpA in the protein profile of R_{low} (as well as their absence from the protein profile of R_{high}) was confirmed by Western blotting. While R_{high} expresses a form of Hlp3 that reacts with anti-HMW3 antiserum, the reaction is not as strong as that observed for R_{low}. This indicates that Hlp3 in R_{high} is aberrant in both molecular mass and in relative abundance compared to R_{low}.

Nucleotide sequencing of *hlp3* and *plpA* indicates that both genes are disrupted in R_{high}. The disruption of *hlp3* is an in-frame deletion resulting in the removal of 18 amino acids from the protein product. This deletion is likely responsible for the altered mobility of Hlp3 in R_{high}. It is noteworthy that this deletion encompasses a large portion of sequence encoding peptide 1, an amino acid stretch shown to bind fibronectin. The 17-bp duplication in *plpA* disrupts the reading frame and results in a premature truncation. This defect would affect only the C-terminal portion of the protein product; however, the visual absence of PlpA when examined by SDS-PAGE, as well as the lack of reactivity in R_{high} to antibodies targeting peptides at both the MID and C-terminal regions of PlpA, indicates that neither truncated nor full-length PlpA protein is present in R_{high}. Despite the lack of translated product, transcriptional analysis demonstrated that R_{low} and R_{high} produce mRNA for both *hlp3* and *plpA*. This indicates that a dysfunction at the translational or posttranslational level is responsible for the reduction and absence of Hlp3 and PlpA, respectively, in R_{high}. Reasons for the apparent instability of PlpA are currently under investigation.

Two peptides selected from regions aligning most closely with annotated fibronectin-binding proteins, one from Hlp3 and one from PlpA, were shown to bind fibronectin in vitro. Peptides 1 and 7 are 60% identical and 80% similar to each other (Fig. 4C). As there is a difference in the reaction intensity of each peptide with fibronectin, the critical residues for these interactions likely include one or more of the similar amino acids.

The current model describing the topology of the proteins comprising the attachment organelle of *M. pneumoniae* indicates that HMW3 is intracellular (39), while the cytadherence-associated protein P65 is surface exposed (32). The *M. gallisepticum* counterparts of these proteins have been implicated in a function that would largely necessitate an extracellular location. We demonstrate that anti-PlpA IgG inhibits binding of fibronectin by viable R_{low}, supporting the predictions that PlpA has an extracellular location and that it binds fibronectin. The degradation of PlpA when whole R_{low} cells are exposed to proteinase K, as well as the ability of anti-PlpA antibodies to bind R_{low} and fix complement, thereby inhibiting growth, provides further evidence of the surface-exposed location of PlpA. Due to the degree of homology that Hlp3 and PlpA share, particularly in the suspected fibronectin-binding domains, we propose that PlpA is responsible for in vivo binding of fibronectin and that the in vitro binding by Hlp3 may be incidental to the homology between the two proteins within the suspected binding domain. These conclusions are further supported by the observation that the predicted fibronectin-binding domain of PlpA (peptide 7) exhibits a stronger interaction with fibronectin than that of the Hlp3 fibronectin-binding domain (peptide 1) and fibronectin. Analogous experiments analyzing the topology of Hlp3 were inconclusive (data not shown); therefore, definitive statements regarding the subcellular location of Hlp3 cannot be made at this time.

The observed topology of PlpA is not consistent with in silico analyses that indicate an intracellular location. Although an extracellular location of P65 has been described for *M. pneumoniae* (16, 32, 36), the mechanism by which it becomes surface exposed is unclear at this point. Neither P65 from *M. pneumoniae* or *M. genitalium* nor PlpA from *M. gallisepticum* possesses any classical transmembrane domains or signal peptides (10, 15, 28). The N terminus of PlpA does, however, possess features typical of membrane proteins, including 10 GG_4 motifs (24, 28). The 10 GG_4 motifs in PlpA occur as 5 expanded motifs (i.e., GxxxGxxxG), as is seen with the vacuolating toxin (VacA) of *Helicobacter pylori*. In the case of VacA, the expanded motif proved essential to interactions with other proteins on the surface of *H. pylori* (17).

We examined the possibility that an atypical transmembrane domain exists to facilitate the surface exposure of PlpA. The expanded motif of GG_4 (GG_4E) was targeted for investigation, due to its predicted properties in PlpA. In each of the five repeats in PlpA, five of the six variable residues are nonpolar. The predicted conformation of PlpA using GOR IV (11) indicates that all occurrences of the motif exist primarily as low-complexity regions (i.e., beta strands) between coiled-coil regions. If a stretch of sequence is not in an alpha-helical conformation, the predicted minimum number of amino acid residues required to span a cell membrane is six (30), making it theoretically possible for the GG_4E peptide to completely traverse a cell membrane. This lack of secondary structure, in conjunction with the hydrophobicity of the sequence in that region, supports the notion that this motif is implicated in anchoring the protein in the cell membrane.

A peptide representing the expanded repeat of GG_4 was shown to incorporate within liposomes and to embed within the *M. gallisepticum* membrane. Detection of this peptide in association with both liposomes and cell membranes represents embedding, rather than nonspecific binding. This is supported by the fact that GG_4E peptides exposed to *M. gallisepticum* cells in the absence of an electrical pulse did not remain in association with the membrane following washes, indicating that this peptide does not bind the cell surface nonspecifically. The lack of positive signal in these experiments also indicates that the streptavidin conjugate alone does not bind the cell surface. Exposure of the streptavidin conjugate to unmodified liposomes eliminated the possibility of signal being generated due to nonspecific binding. The charged, phosphorylated head portions of each phospholipid molecule compose the surface of the liposomes and are therefore unlikely to directly bind peptides that are composed primarily of hydrophobic amino acids. The lack of binding by the hydrophobic II_4 (IPVVI) and GG_4 (GMLAG) peptides provides experimental evidence to support this.

In addition to PlpA, the *M. pneumoniae* protein PdhB (Gen Bank accession no. NP_110080) has been shown to be a surface-exposed fibronectin-binding protein, despite a lack of classical transmembrane domains (7). PdhB also possesses the expanded GG_4 motif, wherein all of the variable residues are hydrophobic. These preliminary data indicate that these regions may be able to serve as atypical transmembrane regions. Further investigation of these motifs within the context of whole proteins will be necessary to gauge their potential as membrane-spanning regions.

The identification of PlpA and Hlp3 as fibronectin-binding proteins suggests that *M. gallisepticum* possesses additional mechanisms potentially associated with virulence that warrant further exploration. The nature of the disease state caused by *M. gallisepticum* is chronic, indicating that the organisms are accomplished at evading the immune system of their host. Although much of this evasion can be attributed to antigenic variation (2, 12, 22), it is possible that a secondary evasive mechanism exists. Evidence suggests that *M. gallisepticum* may enter epithelial cells and exist within them before rapidly exiting (48). In addition, *M. gallisepticum* has been isolated from several mucosal epithelial surfaces including the trachea, lungs, air sacs, sinuses, and ovaries, as well as nonmucosal epithelial surfaces such as the brain and arterial walls (5, 6, 49). The organism clearly has a mechanism(s) by which it travels from one tissue to another that has yet to be described. Fibronectin binding may play a role in the aforementioned activities, thereby contributing to the overall pathogenicity of the organism.

The fibronectin-binding domain of PlpA was shown to interact with the gelatin/heparin-binding domain of fibronectin. This domain is located on the CTD of the molecule, proximal to the site of interaction between fibronectin and integrins (35). Binding of PlpA to the gelatin/heparin-binding domain of fibronectin may allow *M. gallisepticum* to locate closer to the host cell surface, in proximity to the site of extracellular matrix-integrin interactions. PlpA, as the homologue of an *M. pneumoniae* cytoskeletal protein and a fibronectin-binding protein, is a potentially important component of the virulence of *M. gallisepticum*. Although the *M. gallisepticum* homologues of the *M. pneumoniae* tip structure proteins have not been investigated to date, these preliminary studies wherein PlpA and Hlp3 are absent or aberrant in an attenuated strain indicate that the generation of a comparative model of tip structure assembly may be beneficial to facilitating a more thorough understanding of the process of attachment.

ACKNOWLEDGMENTS

We acknowledge Mitchell Balish of the University of Miami of Ohio and Edan Tulman of the University of Connecticut for helpful discussions.

This research was supported by USDA grant 58-1940-0-007.

REFERENCES

1. **Balish, M. F., and D. C. Krause.** 2002. Cytadherence and the cytoskeleton, p. 491–518. *In* S. Razin and R. Herrmann (ed.), Molecular biology and pathogenicity of mycoplasmas. Kluwer Academic/Plenum Publishers, New York, N.Y.
2. **Baseggio, N., M. D. Glew, P. F. Markham, K. G. Whithear, and G. F. Browning.** 1996. Size and genomic location of the pMGA multigene family of *Mycoplasma gallisepticum*. Microbiology **142:**1429–1435.
3. **Bordier, C.** 1981. Phase separation of integral membrane proteins in Triton X-114 solution. J. Biol. Chem. **256:**1604–1607.
4. **Cheng, H. C., M. Abdel-Ghany, R. C. Elble, and B. U. Pauli.** 1998. Lung endothelial dipeptidyl peptidase IV promotes adhesion and metastasis of rat breast cancer cells via tumor cell surface-associated fibronectin. J. Biol. Chem. **273:**24207–24215.
5. **Chin, R. P., B. M. Daft, C. U. Meteyer, and R. Yamamoto.** 1991. Meningoencephalitis in commercial meat turkeys associated with Mycoplasma gallisepticum. Avian Dis. **35:**986–993.
6. **Clyde, W. A., Jr., and L. Thomas.** 1973. Tropism of Mycoplasma gallisepticum for arterial walls. Proc. Natl. Acad. Sci. USA **70:**1545–1549.
7. **Dallo, S. F., T. R. Kannan, M. W. Blaylock, and J. B. Baseman.** 2002. Elongation factor Tu and E1 beta subunit of pyruvate dehydrogenase complex act as fibronectin binding proteins in Mycoplasma pneumoniae. Mol. Microbiol. **46:**1041–1051.
8. **Dehio, C., S. D. Gray-Owen, and T. F. Meyer.** 2000. Host cell invasion by pathogenic Neisseriae. Subcell. Biochem. **33:**61–96.
9. **Dinkla, K., M. Rohde, W. T. Jansen, J. R. Carapetis, G. S. Chhatwal, and S. R. Talay.** 2003. Streptococcus pyogenes recruits collagen via surface-bound fibronectin: a novel colonization and immune evasion mechanism. Mol. Microbiol. **47:**861–869.

10. **Fraser, C. M., J. D. Gocayne, O. White, M. D. Adams, R. A. Clayton, R. D. Fleischmann, C. J. Bult, A. R. Kerlavage, G. Sutton, J. M. Kelley, R. D. Fritchman, J. F. Weidman, K. V. Small, M. Sandusky, J. Fuhrmann, D. Nguyen, T. R. Utterback, D. M. Saudek, C. A. Phillips, J. M. Merrick, J. F. Tomb, B. A. Dougherty, K. F. Bott, P. C. Hu, T. S. Lucier, S. N. Peterson, H. O. Smith, C. A. Hutchison III, and J. C. Venter.** 1995. The minimal gene complement of Mycoplasma genitalium. Science **270:**397–403.
11. **Garnier, J., J. F. Gibrat, and B. Robson.** 1996. GOR method for predicting protein secondary structure from amino acid sequence. Methods Enzymol. **266:**540–553.
12. **Gorton, T. S., and S. J. Geary.** 1997. Antibody-mediated selection of a Mycoplasma gallisepticum phenotype expressing variable proteins. FEMS Microbiol. Lett. **155:**31–38.
13. **Herrmann, M., P. E. Vaudaux, D. Pittet, R. Auckenthaler, P. D. Lew, F. Schumacher-Perdreau, G. Peters, and F. A. Waldvogel.** 1988. Fibronectin, fibrinogen, and laminin act as mediators of adherence of clinical staphylococcal isolates to foreign material. J. Infect. Dis. **158:**693–701.
14. **Hillenkamp, F., and M. Karas.** 1990. Mass spectrometry of peptides and proteins by matrix-assisted ultraviolet laser desorption/ionization. Methods Enzymol. **193:**280–295.
15. **Himmelreich, R., H. Hilbert, H. Plagens, E. Pirkl, B. C. Li, and R. Herrmann.** 1996. Complete sequence analysis of the genome of the bacterium Mycoplasma pneumoniae. Nucleic Acids Res. **24:**4420–4449.
16. **Jordan, J. L., K. M. Berry, M. F. Balish, and D. C. Krause.** 2001. Stability and subcellular localization of cytadherence-associated protein P65 in *Mycoplasma pneumoniae*. J. Bacteriol. **183:**7387–7391.
17. **Kim, S., A. K. Chamberlain, and J. U. Bowie.** 2004. Membrane channel structure of Helicobacter pylori vacuolating toxin: role of multiple GXXXG motifs in cylindrical channels. Proc. Natl. Acad. Sci. USA **101:**5988–5991.
18. **Krause, D. C.** 1996. Mycoplasma pneumoniae cytadherence: unravelling the tie that binds. Mol. Microbiol. **20:**247–253.
19. **Krause, D. C., and M. F. Balish.** 2001. Structure, function, and assembly of the terminal organelle of Mycoplasma pneumoniae. FEMS Microbiol. Lett. **198:**1–7.
20. **Kyte, J., and R. F. Doolittle.** 1982. A simple method for displaying the hydropathic character of a protein. J. Mol. Biol. **157:**105–132.
21. **Laemmli, U. K., and S. F. Quittner.** 1974. Maturation of the head of bacteriophage T4. IV. The proteins of the core of the tubular polyheads and in vitro cleavage of the head proteins. Virology **62:**483–499.
22. **Levisohn, S., R. Rosengarten, and D. Yogev.** 1995. In vivo variation of Mycoplasma gallisepticum antigen expression in experimentally infected chickens. Vet. Microbiol. **45:**219–231.
23. **Ley, D. H., J. E. Berkhoff, and J. M. McLaren.** 1996. Mycoplasma gallisepticum isolated from house finches (Carpodacus mexicanus) with conjunctivitis. Avian Dis. **40:**480–483.
24. **Liu, Y., D. M. Engelman, and M. Gerstein.** 2002. Genomic analysis of membrane protein families: abundance and conserved motifs. Genome Biol. **3:**research0054.1-research0054.12.
25. **Morrissey, J. H.** 2001. Morrissey lab protocol for preparing phospholipid vesicles (SUV) by sonication. [Online.] www.avantilipids.com/pdf/morrissey labprotocolforprepsuvbysonication.pdf.
26. **Nyberg, P., M. Rasmussen, U. Von Pawel-Rammingen, and L. Bjorck.** 2004. SpeB modulates fibronectin-dependent internalization of *Streptococcus pyogenes* by efficient proteolysis of cell-wall-anchored protein F1. Microbiology **150:**1559–1569.
27. **Papazisi, L., S. Frasca, Jr., M. Gladd, X. Liao, D. Yogev, and S. J. Geary.** 2002. GapA and CrmA coexpression is essential for *Mycoplasma gallisepticum* cytadherence and virulence. Infect. Immun. **70:**6839–6845.
28. **Papazisi, L., T. S. Gorton, G. Kutish, P. F. Markham, G. F. Browning, D. K. Nguyen, S. Swartzell, A. Madan, G. Mahairas, and S. J. Geary.** 2003. The complete genome sequence of the avian pathogen Mycoplasma gallisepticum strain R_{low}. Microbiology **149:**2307–2316.
29. **Papazisi, L., K. E. Troy, T. S. Gorton, X. Liao, and S. J. Geary.** 2000. Analysis of cytadherence-deficient, GapA-negative *Mycoplasma gallisepticum* strain R. Infect. Immun. **68:**6643–6649.
30. **Paul, C., and J. P. Rosenbusch.** 1985. Folding patterns of porin and bacteriorhodopsin. EMBO J. **4:**1593–1597.
31. **Pearson, W. R., and D. J. Lipman.** 1988. Improved tools for biological sequence comparison. Proc. Natl. Acad. Sci. USA **85:**2444–2448.
32. **Proft, T., H. Hilbert, G. Layh-Schmitt, and R. Herrmann.** 1995. The proline-rich P65 protein of *Mycoplasma pneumoniae* is a component of the Triton X-100-insoluble fraction and exhibits size polymorphism in the strains M129 and FH. J. Bacteriol. **177:**3370–3378.
33. **Razin, S., D. Yogev, and Y. Naot.** 1998. Molecular biology and pathogenicity of mycoplasmas. Microbiol. Mol. Biol. Rev. **62:**1094–1156.
34. **Secott, T. E., T. L. Lin, and C. C. Wu.** 2004. *Mycobacterium avium* subsp. *paratuberculosis* fibronectin attachment protein facilitates M-cell targeting and invasion through a fibronectin bridge with host integrins. Infect. Immun. **72:**3724–3732.
35. **Sekiguchi, K., and S. Hakomori.** 1980. Functional domain structure of fibronectin. Proc. Natl. Acad. Sci. USA **77:**2661–2665.
36. **Seto, S., G. Layh-Schmitt, T. Kenri, and M. Miyata.** 2001. Visualization of the attachment organelle and cytadherence proteins of *Mycoplasma pneumoniae* by immunofluorescence microscopy. J. Bacteriol. **183:**1621–1630.
37. **Shimoji, Y., Y. Ogawa, M. Osaki, H. Kabeya, S. Maruyama, T. Mikami, and T. Sekizaki.** 2003. Adhesive surface proteins of *Erysipelothrix rhusiopathiae* bind to polystyrene, fibronectin, and type I and IV collagens. J. Bacteriol. **185:**2739–2748.
38. **Sinha, B., P. P. Francois, O. Nusse, M. Foti, O. M. Hartford, P. Vaudaux, T. J. Foster, D. P. Lew, M. Herrmann, and K. H. Krause.** 1999. Fibronectin-binding protein acts as Staphylococcus aureus invasin via fibronectin bridging to integrin $\alpha5\beta1$. Cell. Microbiol. **1:**101–117.
39. **Stevens, M. K., and D. C. Krause.** 1992. *Mycoplasma pneumoniae* cytadherence phase-variable protein HMW3 is a component of the attachment organelle. J. Bacteriol. **174:**4265–4274.
40. **Talay, S. R., A. Zock, M. Rohde, G. Molinari, M. Oggioni, G. Pozzi, C. A. Guzman, and G. S. Chhatwal.** 2000. Co-operative binding of human fibronectin to Sfbl protein triggers streptococcal invasion into respiratory epithelial cells. Cell. Microbiol. **2:**521–535.
41. **Thomas, D. D., J. B. Baseman, and J. F. Alderete.** 1985. Fibronectin mediates Treponema pallidum cytadherence through recognition of fibronectin cell-binding domain. J. Exp. Med. **161:**514–525.
42. **Thomas, D. D., J. B. Baseman, and J. F. Alderete.** 1985. Fibronectin tetrapeptide is target for syphilis spirochete cytadherence. J. Exp. Med. **162:**1715–1719.
43. **Towbin, H., T. Staehelin, and J. Gordon.** 1979. Electrophoretic transfer of proteins from polyacrylamide gels to nitrocellulose sheets: procedure and some applications. Proc. Natl. Acad. Sci. USA **76:**4350–4354.
44. **Troy, K. E.** 1998. Genetic analysis of a MGP1$^-$ high passage *Mycoplasma gallisepticum* strain R. Master's thesis. The University of Connecticut, Storrs, CT.
45. **Tully, J. G., and R. F. Whitcomb.** 1979. The mycoplasmas: human and animal mycoplasmas, vol. 1, p. 2–48. Academic Press, New York, N.Y.
46. **Tuszynski, G. P., T. N. Wang, and D. Berger.** 1997. Adhesive proteins and the hematogenous spread of cancer. Acta Haematol. **97:**29–39.
47. **Willby, M. J., and D. C. Krause.** 2002. Characterization of a *Mycoplasma pneumoniae hmw3* mutant: implications for attachment organelle assembly. J. Bacteriol. **184:**3061–3068.
48. **Winner, F., R. Rosengarten, and C. Citti.** 2000. In vitro cell invasion of *Mycoplasma gallisepticum*. Infect. Immun. **68:**4238–4244.
49. **Yoder, H.** 1978. Diseases of poultry, p. 236–250. Iowa State University Press, Ames, Iowa.

Editor: J. T. Barbieri